Virchows Arch (2010) 457:705–713
DOI 10.1007/s00428-010-0986-5

ORIGINAL ARTICLE

Interaction of Snail and p38 mitogen-activated protein kinase results in shorter overall survival of ovarian cancer patients

Susanne Hipp · Daniela Berg · Bilge Ergin · Tibor Schuster · Alexander Hapfelmeier · Axel Walch · Stefanie Avril · Barbara Schmalfeldt · Heinz Höfler · Karl-Friedrich Becker

Received: 30 June 2010 / Revised: 8 September 2010 / Accepted: 24 September 2010 / Published online: 19 October 2010

Abstract Epithelial ovarian cancer is a highly metastatic disease and the leading cause of death among cancer of the female genital tract. Abnormal epidermal growth factor receptor (EGFR) signalling has been shown to be involved in epithelial–mesenchymal transition (EMT), an early step during metastasis. Additionally, over-expression of the E-cadherin repressor Snail, a key regulator of EMT, has previously been found to be associated with unfavourable prognostic features. Thus, the aim of our study was to elucidate the role of EGFR-dependent signalling pathways for Snail expression in ovarian cancer. For this purpose, we analysed 25 formalin-fixed and paraffin-embedded (FFPE) primary tumours and their corresponding metastases for the expression of 25 signalling pathway molecules by reverse phase protein arrays. We found a significant correlation of Snail with EGFR$^{(Tyr1086)}$ and p38 MAPK$^{(Thr180/Tyr182)}$ in primary ovarian carcinoma and with EGFR$^{(Tyr1086)}$ in their corresponding metastasis. Additionally, we showed that high expression levels of Snail in primary tumours combined with high expression levels of the phosphorylated p38 MAPK$^{(Thr180/Tyr182)}$ in metastasis lead to an increased risk for death in ovarian carcinoma patients. Thus, for future combinatorial cancer therapy, drug combinations that best target the deregulated protein network in each individual patient should be selected.

Keywords Snail · p38 · Ovarian cancer · Reverse phase protein microarray (RPPA) · Formalin-fixed and paraffin-embedded tissues (FFPE)

Electronic supplementary material The online version of this article (doi:10.1007/s00428-010-0986-5) contains supplementary material, which is available to authorized users.

S. Hipp · D. Berg · B. Ergin · S. Avril · H. Höfler · K.-F. Becker (✉)
Institut für Pathologie, Technische Universität München,
Trogerstrasse 18,
81675 Munich, Germany
e-mail: kf.becker@lrz.tum.de

T. Schuster · A. Hapfelmeier
Institut für medizinische Statistik und Epidemiologie, Technische Universität München,
Munich, Germany

A. Walch · H. Höfler
Helmholtz Zentrum München, Deutsches Forschungszentrum für Gesundheit und Umwelt GmbH, Pathologie,
Neuherberg, Germany

B. Schmalfeldt
Frauenklinik und Poliklinik der Technischen Universität München,
Munich, Germany

Introduction

Ovarian cancer is a highly metastatic disease exhibiting one of the leading causes of cancer death among women in the developed world [1, 2]. Unfortunately, this disease is often not diagnosed until in advanced stages (FIGO stages III–IV) and not before metastatic setting of the tumour due to the lack of early-stage detection [3]. It is known that metastasis still represents the major cause of the failure of cancer treatment. Therefore, the identification of molecules or signalling pathways involved in metastasis has high impact for the development of an optimal therapy for cancers for which early-stage detection is still an obstacle. In addition to the clarification of the protein network within primary tumours, a critical question is to what extent signalling pathway changes do occur upon metastasis [4]. Immunohistochemistry (IHC) may not be suitable for the analysis of subtle quantitative changes in multiple classes of proteins taking place simultaneously within a tissue. Hence, for optimal patient selection and therapy, new

techniques being able to detect the entire spectrum of deregulated pathways in tumours before and during treatment are needed in addition to IHC. Reverse phase protein array (RPPA) is a very promising new technology that allows the simultaneous analysis of multiple parameters over time, before and after treatment, between disease and non-disease states and between responders and non-responders. Since formalin fixation and paraffin embedding is the standard method for tissue handling in almost all hospitals worldwide, we performed our profiling studies on formalin-fixed and paraffin-embedded (FFPE) ovarian cancer tissues. In fact, it became possible to successfully extract full-length, immunoreactive proteins from FFPE tissues only recently. Therefore, the extraction of full-length proteins from FFPE tissues [5], which then can be applied for RPPA [5–7], represents a powerful tool for the quantitative analysis of protein-based networks in cancer tissues.

Metastasis of ovarian cancer involves a series of cellular events including cell-to-cell and cell-to-matrix adhesion as well as proteolytic activities leading to shedding and dispersal of malignant cells [8, 9]. The differentiation of epithelial cells towards a mesenchymal state, called epithelial–mesenchymal transition (EMT), has been recognised as a key step during cancer metastasis and is known as vital for the physiology of ovarian surface epithelium as well as for the growth and dissemination of ovarian cancer [1, 10, 11]. Deregulated epidermal growth factor receptor (EGFR) triggers diverse signalling pathways in tumour cells such as the mitogen-activated protein (MAP) kinases [10, 12] and is considered as one of the major causes of tumour progression and metastasis [13]. The EGFR is often mutated or over-expressed in many epithelial cancers including ovarian cancer [14], and its over-expression is associated with more aggressive disease and poor clinical outcome. Recently, it was shown that EGFR activation induces matrix metalloprotease-9 production and promotes migration and invasion in ovarian cancer cells [15]. Additionally, EGFR regulates E-cadherin protein expression. For example, chronic treatment with EGF leads to loss of cell–cell adherence junctions and to the down-regulation of E-cadherin expression on the transcriptional level [16]. Reduction of E-cadherin expression is known to be a hallmark of EMT. Membranous E-cadherin expression can be modified by various mechanisms including gene mutations [17–19], promoter hyper-methylation [19–21], post-translational modifications [22] and transcriptional repression [23–25].

Snail is one of the most prominent transcriptional repressors of E-cadherin. It binds to the E-boxes of the E-cadherin promoter, which represses gene transcription [23, 24]. Snail is regulated on the transcriptional level as well as on the protein level. Glycogen synthase kinase-3β (GSK-3β) and p21-activated kinase (PAK1) control Snails' subcellular localisation and regulate Snail protein stability [26–28]. Previous studies showed that over-expression of Snail in endometrial carcinoma metastases correlates with higher tumour grade and abnormal E-cadherin expression [29]. Additionally, it is known that Snail over-expression is associated with lower overall survival of ovarian cancer patients [30] and that E-cadherin down-regulation is associated with Snail up-regulation in human ovarian cancer [31, 32].

Recently, it was shown that abnormal tyrosine kinase signalling plays a role in the regulation of EMT during development and in cell culture studies [33]. However, studies demonstrating a clear correlation between receptor tyrosine kinase signalling and Snail, a master regulator of EMT, in ovarian cancer is still missing. Given the association between EGFR over-expression and high metastatic potential, we hypothesised that the EGFR pathway may contribute to the regulation of Snail expression in ovarian carcinoma. Here, we show first a high correlation of EGFR-related signalling pathways with Snail protein expression in ovarian carcinoma and an increased risk for death in ovarian carcinoma patients having high expression levels of Snail in primary tumours and the phosphorylated p38 MAPK$^{(Thr180/Tyr182)}$ in metastasis.

Materials and methods

Tissue samples

FFPE tissue samples from a total of 25 patients who had undergone primary surgery for newly diagnosed advanced stage (FIGO IIIC and IV) ovarian carcinoma were included in this study. The clinicopathological characteristics of the patients are summarised in Table 1. The study was approved by the Ethics Committee of the Technical University of Munich, Germany. Only patients without chemotherapy or radiotherapy within 6 months prior to surgery were included in the study. Follow-up data were available for 24 patients, with a median follow-up time of 55 months. The median follow-up was calculated by the inverse Kaplan–Meier approach [34]. During follow-up time, 16 of 24 patients died. From one patient (no. 18), no follow-up data were available. Additionally, we omitted the two cases of serous carcinomas grade 1 (nos. 18 and 25) from all statistical analysis because these cancer types have a very indolent behaviour that is not comparable with the biology of conventional high grade ovarian carcinomas.

Reference haematoxylin/eosin-stained sections of the tissues were histological verified by an experienced pathologist (AW). Only tissues with at least 85% of tumour cells were included in the study. Different areas within each tumour were sampled. Adjacent unstained sections of the same paraffin blocks were used for protein extraction.

Table 1 Clinicopathological characteristics of the ovarian cancer patients used in this study

No.	Subtype	Tumour grade	T	N	M	Localisation metastasis	Figo	Status	Survival/last follow-up (months)	Age
1	Serous	3	3c	1	0	O	3c	Dead	19.7	52.8
2	Serous	3	3c	x	1	O	4	Dead	3.3	80.0
3	Serous	3	3b	1	0	O	3c	Alive	30.6	74.8
4	Serous	2	3c	x	0	O	3c	Dead	26.5	52.1
5	Serous	2	3c	0	0	P	3c	Dead	23.4	69.5
6	Endometrioid	3	3c	1	0	O	3c	Dead	32.4	47.1
7	Serous	3	3c	x	0	O	3c	Alive	0.1	80.2
8	Serous	3	3c	x	1	O	4	Alive	54.7	55.4
9	Serous	3	3c	1	1	L	4	Dead	0.8	49.3
10	Serous	3	3c	x	0	O	3c	Dead	17.9	80.2
11	Endometrioid	3	3c	x	1	O/P	4	Dead	16.2	55.4
12	Serous	3	3c	1	0	P	3c	Alive	56.8	73.6
13	Serous	2	3c	1	0	O	3c	Dead	55.7	29.5
14	Serous	3	3c	1	0	O	3c	Alive	47.7	64.2
15	Serous	3	3c	1	0	O	3c	Dead	14.0	65.3
16	Serous	3	3c	1	x	O	3c	Alive	30.7	68.8
17	Clear cell carcinoma	3	3c	1	0	O	3c	Dead	5.5	58.9
18	Serous	1	3c	x	x	x	3c	n.d.	n.d.	71.4
19	Serous	3	3c	x	1	P	4	Dead	6.4	71.6
20	Serous	2	3c	0	0	O	3c	Dead	50.0	36.9
21	Serous	3	3c	1	0	P	3c	Dead	31.2	41.2
22	Serous	3	3c	x	0	P	3c	Alive	49.2	61.1
23	Serous	3	3c	x	0	O	3c	Dead	17.7	78.2
24	Serous	3	3c	1	0	O	3c	Dead	48.8	48.3
25	Serous	1	3c	x	0	O	3c	Alive	55.0	76.8

Localisation of the metastasis: *L* lymph node metastasis, *O* omentum metastasis, *P* peritoneal metastasis

Protein extraction from formalin-fixed tissue samples

After standard deparaffination of tissue sections (10 μm), proteins were extracted as previously described [5], using the Qproteome FFPE Tissue Kit (Qiagen, Hilden, Germany).

Immunoblotting

Total protein extracts were subjected to sodium dodecyl sulphate-polyacrylamide gel electrophoresis, and blotting was performed on nitrocellulose membranes (Whatman/Schleicher and Schuell, Dassel, Germany). Blots were developed using the ECLPlus and ECLadvance Western Blot Detection Systems (Amersham/GE Healthcare Europe GmbH, Muenchen, Germany).

Reverse phase protein microarray

RPPA was generated using the BioOdyssey™ Calligrapher™ MiniArrayer (Biorad, Muenchen, Germany). For every lysate and every dilution (undiluted, 1:2, 1:4, buffer), three replicates were applied onto a nitrocellulose-coated glass slide (Fast™ Slide, Whatman/Schleicher and Schuell, Dassel, Germany). Lysate microarrays were developed using the ECLPlus and ECLadvance Western Blot Detection System. For estimation of total protein amounts, parallel arrays were stained with Sypro Ruby Protein Blot Stain (Molecular Probes, Eugene, OR, USA) according to the manufacturer's instructions and visualised on an Eagle Eye (Stratagene, La Jolla, CA, USA). Developed films were scanned individually on a scanner (Scanjet 3770, Hewlett-Packard, Hamburg, Germany) with 1,200 dpi and were saved as TIFF files. Density of protein spots was measured using Scion Image (Scion Corporation, Frederick, MA, USA). Relative expression levels of proteins were calculated by normalising to total protein.

Antibodies

Antibodies used for western blot and RPPA are listed in Supplementary Table 1. Before protein profiling, however, the specificities of all antibodies used in protein lysate microarray analysis were first confirmed, as previously

described. (Supplementary Fig. 1). Parts of this figure have been published recently [35].

Hierarchical clustering

Unsupervised hierarchical clustering was performed by using Cluster and Tree View software [36].

Statistical analysis

Correlation analysis

Bivariate relationships of quantitative data were assessed by the Spearman rank correlation coefficient (rho), using SPSS version 16.0 (SPSS, Inc, Chicago, IL, USA). To correct for multiple testing, Bonferroni adjustment was conducted in the multiple correlation analyses regarding Snail to warrant a global significance level of 5%.

Survival analysis

Statistical analyses on patient survival were carried out with the software package R Version 2.7.1.

As the main interest was on examining the influence of risk factors on survival, Cox proportional hazard models were fit to the data. Hazard ratios describing the factorial change of risk by a one-point increment on the scale of a risk factor were calculated and reported with 95% confidence intervals (CI). As the biological pathway suggested relations between several factors regarding survival, interaction terms were included in the model process. The introduction of interactions allows the observer to examine mutual effects of risk factors. To illustrate the examined influence on risk and therefore facilitate the interpretation of the model parameters, surface plots for the hazard ratio were created.

Statistical survival analyses were conducted at a 0.05 level of significance. Statistical analysis on prognosis is based on the data of primary tumours and metastasis.

Results

Reverse phase protein microarray technology

The RPPA represents a very promising new high-throughput technology for signalling pathway profiling over time, before and after treatment, between disease and non-disease states and between responders and non-responders. This method allows analysis of multiple samples for the expression of one protein under the same experimental conditions in parallel. Moreover, it is suited for signal transduction profiling of small numbers of cultured cells or cells isolated by laser capture microdissection from human biopsies. After protein extraction from FFPE tissues, each patient sample is arrayed in triplicates on nitrocellulose-coated slides in a miniature dilution curve. Thus, each analyte/antibody combination can be analysed in the linear dynamic range. Then, the density of protein spots is measured. In addition to applying the detection antibody, one or more slides spotted in parallel are stained with a total protein detection reagent (e.g. SYPRO® Ruby staining solution). This step is necessary for normalisation of the signals obtained by the antibodies to total protein (Fig. 1).

Profiling of signalling proteins of primary tumours and metastasis of ovarian cancer patients using RPPA

Cancer cells of epithelial origin, including ovarian cancer cells, undergo EMT as an early event during metastasis. EGFR over-expression and deregulated signalling pathways are considered to be linked to cancer invasion/metastasis. But the specific involvement of EGFR signalling in EMT of ovarian carcinoma remains elusive.

Therefore, we investigated whether EGFR activation is involved in Snail regulation in primary tumours and/or metastases of ovarian cancer. To this end, we performed RPPA analysis with protein extracts from 23 FFPE primary tumours and their corresponding metastases generating a tumour specific protein network portrait. Although patient-specific signalling is apparent, the protein expression can be divided each into two groups (Fig. 2a). In the primary tumours, the phosphorylated forms of HER2$^{(Tyr1248)}$, p38 MAPK$^{(Thr180/Tyr182)}$ and PAK1$^{(Thr212)}$ are located in one cluster together with the active form of EGFR$^{(Tyr1086)}$ and Snail, indicating that these molecules may be involved in the EGF-dependent regulation of Snail. In metastases, however, only the phosphorylated forms of STAT3$^{(Tyr705)}$ and HSP27$^{(Ser82)}$ seem to be involved in the EGFR-dependent regulation of Snail expression (Fig. 2b). Neither in primary tumours nor in metastasis was a statistically significant association between Snail expression and clinicopathological parameters found (Table 2).

To underpin the observations from our cluster analysis, we additionally performed Spearman correlation (Table 3). Again, we found Snail correlating with the active forms of EGFR$^{(Tyr1086)}$ and p38 MAPK$^{(Thr180/Tyr182)}$ in primary ovarian carcinoma and with phospho-EGFR$^{(Tyr1086)}$ in their corresponding metastasis.

In further Spearman correlation analysis, we evaluated signalling networks related to primary tumours and their corresponding metastasis and EMT. Again, we could detect differences between primary tumours and metastasis. Only the expression of 11 of the 25 proteins analysed correlated statistically significant in primary tumours and metastases (Table 4).

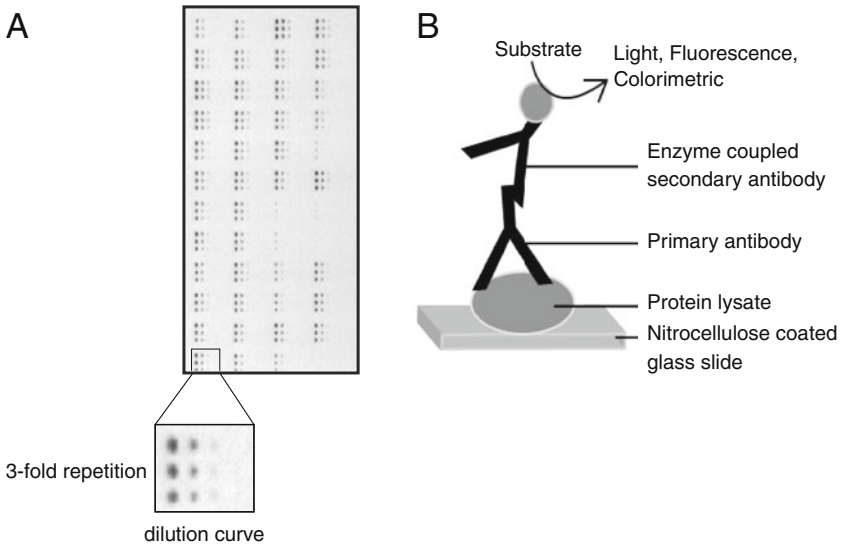

Fig. 1 Reverse phase protein microarray. **a** Protein lysates from FPPE cancer tissue samples were spotted on a nitrocellulose-coated glass slide, followed by incubation with the primary antibody. Per lysate, a 3-fold dilution curve in three replicates was spotted. For normalisation of the antibody signals to total protein, the slide was stained with Sypro Ruby reagent. **b** Patient samples are arrayed onto a nitrocellulose-coated glass slide and incubated with a primary antibody of interest. Detection is carried out by using an enzyme coupled secondary antibody together with its target substrate

Interaction of Snail and p38 mitogen-activated protein kinase leads to shorter overall survival of ovarian cancer patients

So far, we documented a strong correlation between Snail and the phosphorylated forms of EGFR$^{(Tyr1086)}$ and p38 MAPK$^{(Thr180/Tyr182)}$ in primary ovarian tumours. Now, we asked whether specific combinations of Snail and these proteins have a prognostic value. In Cox hazard regression analyses summarised in Table 5, patients with high expression levels of both Snail and the phosphorylated form of p38 MAPK showed a significantly higher risk of death.

The first two models show the results of the univariable analyses of Snail and E-cadherin in primary

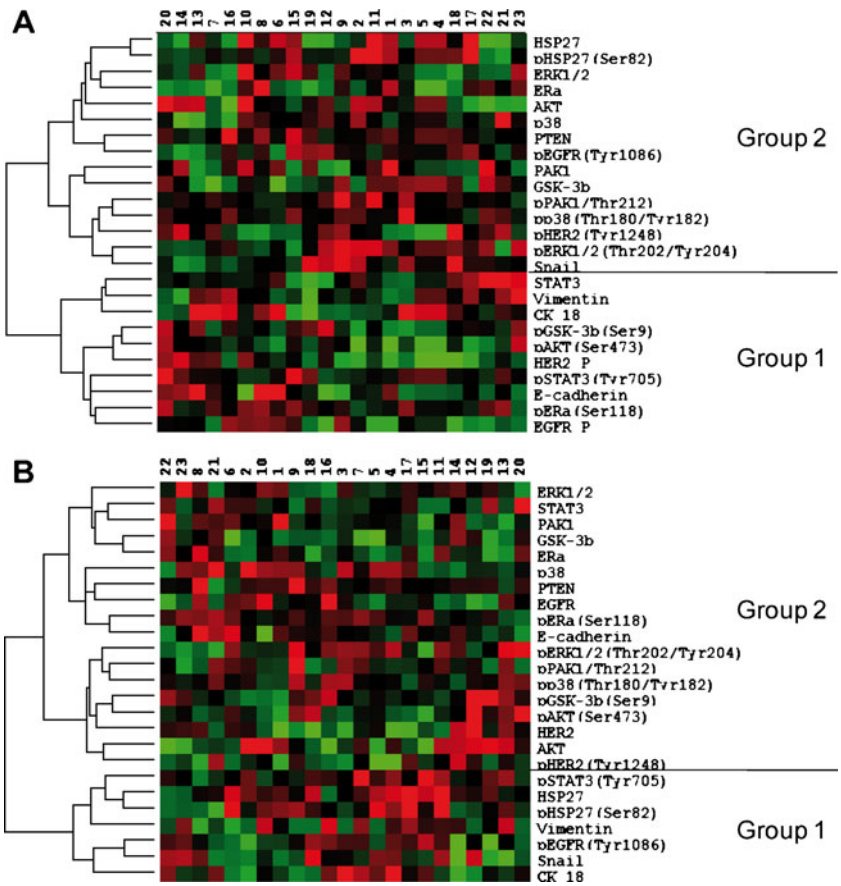

Fig. 2 Protein network portrait. Twenty-five proteins were used in the analysis of primary tumours (**a**) and metastases (**b**). The patients are numbered in the *horizontal axis*, and the protein expression is on the *vertical axis*. Higher protein expression levels are represented in *red*; lower levels, in *green*

Table 2 Median and interquartile range of Snail in quantitative clinicopathological parameters for primary tumours and metastasis

		Snail			
		N	Median	(range)/[IQR][a]	*p*
Primary tumours					
Grade	2	4	0.09	(0.08; 1.26)	0.218
	3	19	0.40	[0.23; 0.69]	
T	3b	1	0.79		–[b]
	3c	22	0.32	[0.12; 0.66]	
N	0	2	0.68	(0.09; 1.26)	–[b]
	1	12	0.29	[0.15; 0.77]	
	x	9	0.40	(0.08; 0.76)	
M	0	17	0.24	[0.10; 0.73]	0.164
	1	5	0.44	(0.33; 1.10)	
	x	1	0.42		
Figo	3c	18	0.26	[0.10; 0.71]	0.174
	4	5	0.44	(0.33; 1.10)	
Subtype	1	19	0.33	[0.10; 0.76]	–[b]
	2	2	0.31	(0.21; 0.40)	
	3	2	0.45	(0.30; 0.60)	
Age		23	Spearman's rho, +0.124		0.573
Metastasis					
Grade	2	4	0.27	(0.10; 0.39)	0.054
	3	19	0.47	[0.27; 0.64]	
T	3b	1	0.46		–[b]
	3c	22	0.42	[0.26; 0.63]	
N	0	2	0.27	(0.15; 0.39)	–[b]
	1	12	0.37	[0.24; 0.63]	
	x	9	0.47	(0.26; 0.96)	
M	0	17	0.38	[0.25; 0.55]	0.164
	1	5	0.58	(0.26; 0.81)	
	x	1	0.64		
Figo	3c	18	0.39	[0.25; 0.62]	0.199
	4	5	0.58	(0.26; 0.81)	
Subtype	1	19	0.44	[0.26; 0.63]	–[b]
	2	2	0.54	(0.26; 0.81)	
	3	2	0.38	(0.29; 0.47)	
Age		23	Spearman's rho, + 0.32		0.138

For continuous variables, Spearman correlation coefficient is given

[a] Interquartile range (*IQR*) instead of range was reported for group sample sizes ≥10

[b] No group comparisons were conducted because of insufficient group sample sizes

tumours, revealing that there is no evidence for a single significant impact of Snail (p value=0.790) and E-cadherin (p=0.156) on the risk of death. The 95% confidence intervals of the hazard ratio estimations show that the factorial risk increment (for a one-unit increase of Snail/E-cadherin) in the underlying population have to be expected in a range 0.22 to 3.22 (Snail) and 0.12 to 1.40 (E-cadherin) with a probability of 95%. If there was a statistically significant association of Snail or E-cadherin and survival, the critical value of one would not be included in these intervals.

As the biological pathway suggested relations between Snail of the primary tumour and the phosphorylated form of

Table 3 Spearman rank correlations (rho) relating Snail expression and expression of various proteins in primary tumours and their corresponding metastases

Protein	Rho	*p* value
Primary tumour		
pEGFR$^{(Tyr1086)}$	**0.874**	**<0.0001**
pHER2$^{(Tyr1248)}$	0.629	0.0324
pp38$^{(Thr180/Tyr182)}$	**0.708**	**0.0038**
pPAK1$^{(Thr212)}$	0.693	0.00625
Metastasis		
pEGFR$^{(Tyr1086)}$	**0.760**	**0.0006**
pHSP27$^{(Ser82)}$	0.148	>0.9999
pSTAT3$^{(Tyr705)}$	0.323	>0.9999

Significant at a Bonferroni-adjusted level of significance p<0.006

Table 4 Spearman rank correlation (rho): protein expression in primary tumour versus metastases

Protein	Rho	*p* value
pAKT$^{(Ser473)}$	**0.734**	**<0.001**
AKT	**0.746**	**<0.001**
Cytokeratin18	0.590	0.003
E-cadherin	0.480	0.020
pEGFR$^{(Tyr1086)}$	0.482	0.020
EGFR	**0.656**	**0.001**
pER$\alpha^{(Ser118)}$	0.527	0.010
ERα	**0.800**	**<0.001**
pERK1/2$^{(Thr202/Tyr204)}$	0.051	0.818
ERK1/2	**0.673**	**<0.001**
pGSK-3$\beta^{(Ser9)}$	**0.858**	**<0.001**
GSK-3β	**0.635**	**0.001**
pHER2$^{(Tyr1248)}$	0.615	0.002
HER2	**0.658**	**0.001**
pHSP27$^{(Ser82)}$	0.569	0.005
HSP27	0.556	0.006
pp38$^{(Thr180/Tyr182)}$	**0.785**	**<0.001**
p38	0.445	0.033
pPAK1$^{(Thr212)}$	**0.704**	**<0.001**
PAK1	0.542	0.008
PTEN	**0.735**	**<0.001**
pSTAT-3$^{(Tyr705)}$	0.468	0.024
STAT-3	**0.701**	**<0.001**
Snail	0.404	0.056
Vimentin	0.612	0.002

Statistical significant at a Bonferroni-adjusted level of significance of 0.0018

Table 5 Cox proportional hazard models for the factors Snail, E-cadherin, and interaction of Snail with pp38$^{(Thr180/Tyr182)}$ in primary tumours and metastasis

Model		Coefficient	Hazard ratio	95% CI		*p* value
				Hazard ratio		
				Lower	Upper	
1	Snail	−0.18	0.83	0.22	3.22	0.790
2	E-cadherin	−0.86	0.42	0.12	1.40	0.156
3	Snail	−4.80	0.0083	0.00014	0.4875	0.021
	pp38$^{(Thr180/Tyr182)}$	−0.702[a]	0.496	0.282	0.872	0.015
	Interaction	1.289[b]	3.630	1.318	9.995	0.012[c]

[a] Per an absolute increment of pp38$^{(Thr180/Tyr182)}$ of 0.10

[b] Per an absolute increment of [Snail×10×pp38$^{(Thr180/Tyr182}$)] of one

[c] Significant at a 5% significance level

p38 MAPK$^{(Thr180/Tyr182)}$ of the metastasis, an interaction term was included in the model which is displayed by model 3 (Table 5). In addition to each risk factor's contribution to the hazard ratio, this interaction term incorporates a change of risk by different parameter constellations. All coefficient *p* values are lower than the 5% significance level. Thus, there is a reasonable evidence that an individual's hazard can be explained by Snail, pp38 MAPK$^{(Thr180/Tyr182)}$, and their interaction. To assess the hazard ratio of an individual in comparison with a person with an expression of Snail=0 and pp38 MAPK$^{(Thr180/Tyr182)}$=0 (reference person), one has to solve the equation hazard ratio=exp(−4.80×Snail−7.00×pp38 MAPK$^{(Thr180/Tyr182)}$+12.81×Snail×pp38$^{(Thr180/Tyr182)}$). To facilitate the interpretation of this relationship, the hazard ratio is illustrated in (Fig. 3). The illustration reveals that high values of both Snail and pp38$^{(Thr180/Tyr182)}$ lead to a high risk for death. A low value in one factor combined with a high value in the other factor will produce a low likelihood ratio.

Discussion

Metastasis is still a major barrier of cancer therapy and represents furthermore one of the primary causes of mortality in many cancers, including ovarian carcinoma. Therefore, it is crucial to understand the biology of cancer cells with high metastatic potential to identify tumours that are likely to undergo metastasis. This would be inalienable to improve current cancer therapies. Additionally, it is known that tumours with deregulated EGFR pathways exhibit a high potential to undergo invasion and migration. However, the specific involvement of EGFR in EMT, an early event during metastasis, and tumour invasion remains elusive [16]. Thus, the current study was undertaken to elucidate whether EGFR-related signalling pathways may contribute to the regulation of the EMT key regulator Snail.

Until now, IHC is routinely used for protein analysis in FFPE cancer tissues. This technique combines anatomical, immunological, and biochemical methods for the identification of specific tissue components via antigen/antibody reaction. Additionally, IHC is an excellent detection technique and has the tremendous advantage of being able to show exactly where a given protein is located within the tissue. However, its major disadvantage is that unlike RPPA, precise protein quantification is difficult and

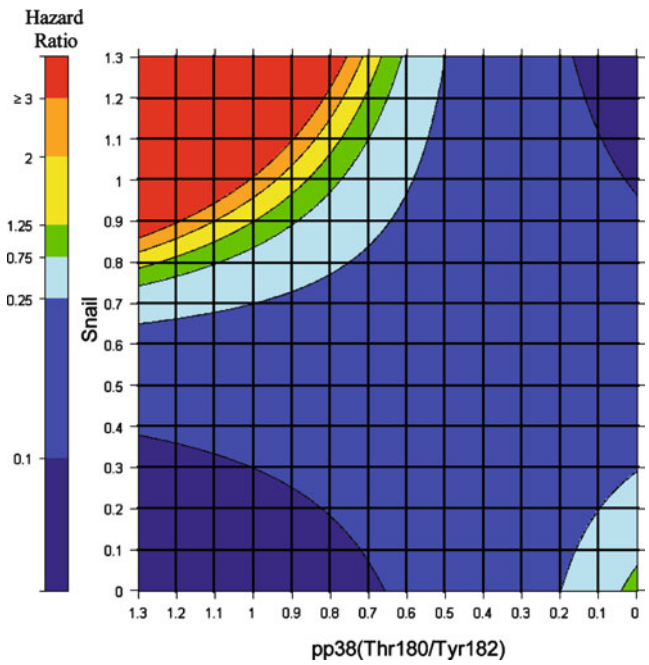

Fig. 3 Estimated hazard ratio in depending on the interaction of Snail and pp38 $^{(Thr180/Tyr182)}$. *Colours* indicate the magnitude of the hazard ratio, which is calculated in reference to the risk of death associated with a zero expression of both Snail and pp38$^{(Thr180/Tyr182)}$

depends in part on the observer. Thus, RPPA has some advantages over IHC. For example, RPPA allows fast analysis of many protein markers in parallel, and this technique is also compatible with low sample volume. Furthermore, in our group, we established a method to standardise and quantify protein expression in patients by the use of purified proteins allowing the determination of protein expression more precisely than it is possible by IHC [7]. Therefore, RPPA is expected to bear advantages for patient and therapy selection, although the correlation between protein abundance and histology is lost. Previous experiments showed that protein expression (e.g. HER2) correlated very well in the RPPA analysis when compared with the "gold standard" IHC, even in small tissue samples such as biopsies [5]. Thus, these results indicate that RPPA technology can reliably be used for biomarker assessment.

In this study, we generated a tumour-specific signalling network portrait of 23 FFPE primary ovarian carcinomas and their corresponding metastasis using RPPA. Consistent with previous results [4], we demonstrated clear differences in protein expression profiles of primary tumours and their metastases (Fig. 2a, b). However, in this context, the specific metastatic process of ovarian cancer should be considered. Both parallel and linear developments of ovarian and extra-ovarian manifestations are possible. Therefore, differences in protein expression observed in this study could be explained by these two cancer progression models. For example, cases that show clear differences in signalling pathways may be generated in parallel. Therefore, these findings indicate the need to additionally compare signalling pathway activity between primary tumours and metastases to understand signal transduction of the tumour within its metastatic microenvironment. Thus, for targeted therapy decisions and optimal patient selections, it is crucial to include patients' metastatic lesions also.

Here, we found Snail significantly correlating with the active forms of EGFR$^{(Tyr1086)}$ and p38 MAPK$^{(Thr180/Tyr182)}$ in primary ovarian carcinomas and with phosphor-EGFR$^{(Tyr1086)}$ in the metastasis. These results are in line with recent reports that described these molecules to play a role in the regulation of Snail. For example, p38 MAPK and ERK1/2 have been shown to act as mediators of Snail and Slug expression after UV exposure in keratinocytes [37]. PAK1 promotes Snail's nuclear accumulation and consequently its repressor activity in human breast cancer [27].

We also asked whether signalling pathways regulating Snail would be of prognostic value. Applying Cox proportional hazard models, we found a statistically significant association between the interaction of the phosphorylated form of p38 MAPK$^{(Thr180/Tyr182)}$ and Snail, and worse overall survival prognosis. This indicates that up-regulation of Snail via p38 MAPK leads to an adverse clinical outcome for ovarian cancer patients. Since the available sample size was rather small and therefore an overly optimistic fit in the survival analysis cannot be excluded, further studies with sufficient sample sizes should be performed to confirm our results. However, the ranges of the 95% confidence intervals of the Cox regression equation, which reflect the uncertainty by sample size, should be considered in the application of our proposed prediction model.

To conclude, our results showed an EGFR-dependent up-regulation of Snail expression in ovarian carcinoma. Additionally, we found for the first time that co-over-expression of phospho-p38 MAPK$^{(Thr180/Tyr182)}$ in metastatic lesions and Snail in primary tumours results in reduced overall survival in patients with ovarian cancer. Thus, for future combinatorial cancer therapy, drug combinations that best target the deregulated protein network in each individual patient should be selected.

Acknowledgements The authors wish to thank Christa Schott for excellent technical assistance. This study is supported by the German Federal Ministry of Education and Research (BMBF) grant no. 01GR0805 to KFB and the Deutsche Forschungsgemeinschaft [*DFG*, grant number BE1501/3-2] to KFB and HH.

Conflict of interest KFB is a named inventor of a patent related to protein extraction from formalin-fixed tissues. He had full access to all of the data in this study and takes complete responsibility for the integrity of the data and the accuracy of the data analysis. Qiagen GmbH, the owner of the patent, did not assert control over the authors' right to publish.

References

1. Ahmed N, Thompson EW, Quinn MA (2007) Epithelial–mesenchymal interconversions in normal ovarian surface epithelium and ovarian carcinomas: an exception to the norm. J Cell Physiol 213:581–588
2. Parkin DM, Bray F, Ferlay J, Pisani P (2005) Global cancer statistics, 2002. CA Cancer J Clin 55:74–108
3. Vergara D, Merlot B, Lucot JP, Collinet P, Vinatier D, Fournier I, Salzet M (2010) Epithelial–mesenchymal transition in ovarian cancer. Cancer Lett 291:59–66
4. Sheehan KM, Calvert VS, Kay EW, Lu FD, Espina V, Aquino J, Speer R, Araujo R, Mills GB, Liotta LA, Petricoin EF 3rd, Wulfkuhle JD (2005) Use of reverse phase protein microarrays and reference standard development for molecular network analysis of metastatic ovarian carcinoma. Mol Cell Proteomics 4:346–355
5. Becker KF, Schott C, Hipp S, Metzger V, Porschewski P, Beck R, Nahrig J, Becker I, Hofler H (2007) Quantitative protein analysis from formalin-fixed tissues: implications for translational clinical research and nanoscale molecular diagnosis. J Pathol 211:370–378
6. Paweletz CP, Charboneau L, Bichsel VE, Simone NL, Chen T, Gillespie JW, Emmert-Buck MR, Roth MJ, Petricoin IE, Liotta LA (2001) Reverse phase protein microarrays which capture disease progression show activation of pro-survival pathways at the cancer invasion front. Oncogene 20:1981–1989

7. Berg D, Hipp S, Malinowsky K, Bollner C, Becker KF (2010) Molecular profiling of signalling pathways in formalin-fixed and paraffin-embedded cancer tissues. Eur J Cancer 46:47–55
8. Geho DH, Bandle RW, Clair T, Liotta LA (2005) Physiological mechanisms of tumor-cell invasion and migration. Physiology (Bethesda) 20:194–200
9. Thompson EW, Newgreen DF, Tarin D (2005) Carcinoma invasion and metastasis: a role for epithelial–mesenchymal transition? Cancer Res 65:5991–5995, discussion 5995
10. Ahmed N, Maines-Bandiera S, Quinn MA, Unger WG, Dedhar S, Auersperg N (2006) Molecular pathways regulating EGF-induced epithelio-mesenchymal transition in human ovarian surface epithelium. Am J Physiol Cell Physiol 290:C1532–C1542
11. Bagnato A, Rosano L (2007) Epithelial–mesenchymal transition in ovarian cancer progression: a crucial role for the endothelin axis. Cells Tissues Organs 185:85–94
12. Yarden Y, Shilo BZ (2007) SnapShot: EGFR signaling pathway. Cell 131:1018
13. Lo HW, Hsu SC, Xia W, Cao X, Shih JY, Wei Y, Abbruzzese JL, Hortobagyi GN, Hung MC (2007) Epidermal growth factor receptor cooperates with signal transducer and activator of transcription 3 to induce epithelial–mesenchymal transition in cancer cells via up-regulation of TWIST gene expression. Cancer Res 67:9066–9076
14. Psyrri A, Kassar M, Yu Z, Bamias A, Weinberger PM, Markakis S, Kowalski D, Camp RL, Rimm DL, Dimopoulos MA (2005) Effect of epidermal growth factor receptor expression level on survival in patients with epithelial ovarian cancer. Clin Cancer Res 11:8637–8643
15. Cowden Dahl KD, Symowicz J, Ning Y, Gutierrez E, Fishman DA, Adley BP, Stack MS, Hudson LG (2008) Matrix metalloproteinase 9 is a mediator of epidermal growth factor-dependent e-cadherin loss in ovarian carcinoma cells. Cancer Res 68:4606–4613
16. Lu Z, Ghosh S, Wang Z, Hunter T (2003) Downregulation of caveolin-1 function by EGF leads to the loss of E-cadherin, increased transcriptional activity of beta-catenin, and enhanced tumor cell invasion. Cancer Cell 4:499–515
17. Becker KF, Atkinson MJ, Reich U, Becker I, Nekarda H, Siewert JR, Hofler H (1994) E-cadherin gene mutations provide clues to diffuse type gastric carcinomas. Cancer Res 54:3845–3852
18. Berx G, Becker KF, Hofler H, van Roy F (1998) Mutations of the human E-cadherin (CDH1) gene. Hum Mutat 12:226–237
19. Machado JC, Oliveira C, Carvalho R, Soares P, Berx G, Caldas C, Seruca R, Carneiro F, Sobrinho-Simoes M (2001) E-cadherin gene (CDH1) promoter methylation as the second hit in sporadic diffuse gastric carcinoma. Oncogene 20:1525–1528
20. Grady WM, Willis J, Guilford PJ, Dunbier AK, Toro TT, Lynch H, Wiesner G, Ferguson K, Eng C, Park JG, Kim SJ, Markowitz S (2000) Methylation of the CDH1 promoter as the second genetic hit in hereditary diffuse gastric cancer. Nat Genet 26:16–17
21. Liu FS (2007) Molecular carcinogenesis of endometrial cancer. Taiwan J Obstet Gynecol 46:26–32
22. Rashid MG, Sanda MG, Vallorosi CJ, Rios-Doria J, Rubin MA, Day ML (2001) Posttranslational truncation and inactivation of human E-cadherin distinguishes prostate cancer from matched normal prostate. Cancer Res 61:489–492
23. Batlle E, Sancho E, Franci C, Dominguez D, Monfar M, Baulida J, Garcia De Herreros A (2000) The transcription factor Snail is a repressor of E-cadherin gene expression in epithelial tumour cells. Nat Cell Biol 2:84–89
24. Cano A, Perez-Moreno MA, Rodrigo I, Locascio A, Blanco MJ, del Barrio MG, Portillo F, Nieto MA (2000) The transcription factor Snail controls epithelial–mesenchymal transitions by repressing E-cadherin expression. Nat Cell Biol 2:76–83
25. Hemavathy K, Ashraf SI, Ip YT (2000) Snail/slug family of repressors: slowly going into the fast lane of development and cancer. Gene 257:1–12
26. Schlessinger K, Hall A (2004) GSK-3beta sets Snail's pace. Nat Cell Biol 6:913–915
27. Yang Z, Rayala S, Nguyen D, Vadlamudi RK, Chen S, Kumar R (2005) Pak1 phosphorylation of Snail, a master regulator of epithelial-to-mesenchyme transition, modulates Snail's subcellular localization and functions. Cancer Res 65:3179–3184
28. Zhou BP, Deng J, Xia W, Xu J, Li YM, Gunduz M, Hung MC (2004) Dual regulation of Snail by GSK-3beta-mediated phosphorylation in control of epithelial–mesenchymal transition. Nat Cell Biol 6:931–940
29. Blechschmidt K, Kremmer E, Hollweck R, Mylonas I, Hofler H, Kremer M, Becker KF (2007) The E-cadherin repressor Snail plays a role in tumor progression of endometrioid adenocarcinomas. Diagn Mol Pathol 16:222–228
30. Blechschmidt K, Sassen S, Schmalfeldt B, Schuster T, Hofler H, Becker KF (2008) The E-cadherin repressor Snail is associated with lower overall survival of ovarian cancer patients. Br J Cancer 98:489–495
31. Elloul S, Silins I, Trope CG, Benshushan A, Davidson B, Reich R (2006) Expression of E-cadherin transcriptional regulators in ovarian carcinoma. Virchows Arch 449:520–528
32. Imai T, Horiuchi A, Wang C, Oka K, Ohira S, Nikaido T, Konishi I (2003) Hypoxia attenuates the expression of E-cadherin via up-regulation of SNAIL in ovarian carcinoma cells. Am J Pathol 163:1437–1447
33. Larue L, Bellacosa A (2005) Epithelial–mesenchymal transition in development and cancer: role of phosphatidylinositol 3' kinase/AKT pathways. Oncogene 24:7443–7454
34. Schemper M, Smith TL (1996) A note on quantifying follow-up in studies of failure time. Control Clin Trials 17:343–346
35. Hipp S, Walch A, Schuster T, Losko S, Laux H, Bolton T, Hofler H, Becker KF (2009) Activation of epidermal growth factor receptor results in Snail protein but not mRNA over-expression in endometrial cancer. J Cell Mol Med 13:3858–3867
36. Eisen MB, Spellman PT, Brown PO, Botstein D (1998) Cluster analysis and display of genome-wide expression patterns. Proc Natl Acad Sci USA 95:14863–14868
37. Hudson LG, Choi C, Newkirk KM, Parkhani J, Cooper KL, Lu P, Kusewitt DF (2007) Ultraviolet radiation stimulates expression of Snail family transcription factors in keratinocytes. Mol Carcinog 46:257–268